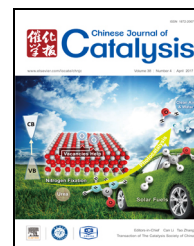


available at www.sciencedirect.comjournal homepage: www.elsevier.com/locate/chnjc

Article

CO₂ hydrogenation to methanol over Cu/Zn/Al/Zr catalysts prepared by liquid reduction

Xiaosu Dong^{a,b}, Feng Li^{a,*}, Ning Zhao^{a,c}, Yisheng Tan^{a,c}, Junwei Wang^{a,c}, Fukui Xiao^{a,c}^a State Key Laboratory of Coal Conversion, Institute of Coal Chemistry, Chinese Academy of Sciences, Taiyuan 030001, Shanxi, China^b University of Chinese Academy of Sciences, Beijing 100049, China^c National Engineering Research Center for Coal-Based Synthesis, Institute of Coal Chemistry, Chinese Academy of Sciences, Taiyuan 030001, Shanxi, China

ARTICLE INFO

Article history:

Received 18 December 2016

Accepted 23 January 2017

Published 5 April 2017

Keywords:

Liquid reduction method

Cu/Zn/Al/Zr catalyst

Carbon dioxide hydrogenation

Methanol

ABSTRACT

Cu/Zn/Al/Zr catalysts containing Cu in three valence states (Cu²⁺, Cu⁺ and Cu⁰) were prepared using a liquid reduction method and subsequently calcined at different temperatures. The effects of the calcination temperature on the catalyst structure, interactions among components, reducibility and dispersion of Cu species, surface properties and exposed Cu surface area were systematically investigated. These materials were also applied to the synthesis of methanol via the hydrogenation of CO₂. The results show that a large exposed Cu surface area promotes catalytic CO₂ conversion and that there is a close correlation between the Cu⁺/Cu⁰ ratio and the selectivity for methanol. A calcination temperature of 573 K was found to produce a Cu/Zn/Al/Zr catalyst exhibiting the maximum activity during the synthesis of methanol.

© 2017, Dalian Institute of Chemical Physics, Chinese Academy of Sciences.

Published by Elsevier B.V. All rights reserved.

1. Introduction

Since global warming caused by the continually increasing CO₂ concentration in the atmosphere is threatening human survival, new technologies based on CO₂ capture and utilization have recently received much attention. The conversion of CO₂ to useful chemicals and fuels may be one of the most promising approaches to mitigating this problem [1]. Methanol, due to its importance in chemical industries and its potential as an environmentally friendly energy carrier, has become the preferred conversion product [2,3]. Therefore, CO₂ catalytic conversion to methanol is a key research topic, along with the optimization of catalysts for this purpose.

Cu-based catalysts obtained from conventional co-precipitation methods are widely used for the synthesis of methanol from CO₂/H₂ [4,5]. However, because of the low melting point

(1356 K) and low Tammann temperature (678 K) of copper, the aggregation of metallic copper particles during the high temperature calcination, reduction and reaction processes have become significant challenges [6,7]. Metallic Cu catalysts are typically prepared by reducing CuO with H₂ [8], although this involves a highly exothermic reaction and thus there is the potential for a runaway reaction. In addition, the high temperatures applied during this process (473 to 623 K) can accelerate the agglomeration of Cu species and thus decrease the efficiency of the active catalytic sites [9]. There has recently been interest in applying a liquid reduction method to the preparation of Cu-based catalysts, because this method is rapid and readily controlled in comparison to conventional gas phase reduction with H₂ [10–12]. Liquid reduction with NaBH₄ is normally carried out at low temperature, thus reducing the agglomeration of Cu species and producing catalysts with smaller metallic

* Corresponding author. Tel/Fax: +86-351-4041153; E-mail: lifeng2729@sxicc.ac.cn

This work was supported by the Key Science and Technology Program of Shanxi Province, China (MD2014-10), the National Key Technology Research and Development Program (2013BAC11B00), and the National Natural Science Foundation of China (21343012).

DOI: 10.1016/S1872-2067(17)62793-1 | <http://www.sciencedirect.com/science/journal/18722067> | Chin. J. Catal., Vol. 38, No. 4, April 2017

particles [10]. Our own group formerly performed a systematic study of the difference between the co-precipitation and liquid reduction methods with regard to the subsequent efficiency of catalytic CO₂ conversion to methanol. This prior work demonstrated that a catalyst fabricated by the liquid reduction method contained smaller Cu particles and exhibited superior catalytic activity and better selectivity for methanol [12].

The oxidation states of Cu species are susceptible to change during sintering and calcination processes. Many research reports have described the effects of calcination temperature on the structure and catalytic performance over conventional Cu-based catalysts containing only Cu²⁺ [13–16]. However, to the best of our knowledge, there have been no reports concerning the effects of calcination temperature on Cu-based catalysts containing Cu species in more highly reduced states. In view of the ready aggregation of metallic copper particles, catalysts prepared by liquid reduction may exhibit complicated changes with elevation of the calcination temperature. Hence, it would be of significant interest to carry out systematic research into the properties and catalytic performance of catalysts prepared by the liquid reduction method while varying the calcination temperature.

In the present work, Cu/Zn/Al/Zr precursors were prepared by the liquid reduction method and then calcined at different temperatures. These catalysts were subsequently applied to the synthesis of methanol from CO₂/H₂ and also characterized by X-ray diffraction (XRD), N₂ physisorption, scanning electron microscopy (SEM), N₂O chemisorption, X-ray photoelectron spectroscopy (XPS), temperature-programmed reduction (TPR), and CO₂ temperature-programmed desorption (TPD). The effects of calcination temperature on the physicochemical properties and catalytic performance of these catalysts are discussed in detail.

2. Experimental

2.1. Preparation of catalysts

Cu-based catalysts having the composition ratio Cu²⁺:Zn²⁺:Al³⁺:Zr⁴⁺ = 6:3:0.5:0.5 were prepared by the liquid reduction method. In a typical process, a solution of mixed metal nitrates (1.0 mol/L, 100 mL) and a solution of the Na₂CO₃ precipitant (1.2 mol/L) were added dropwise to deionized water (100 mL) with stirring at 338 K and at a constant pH value of 7.0 ± 0.2. NaBH₄ (B/Cu molar ratio = 5, 11.35 g) was dissolved in a NaOH solution (0.1 mol/L, 100 mL) to prepare a reducing agent solution. After removing air from the reaction mixture, the reducing agent solution was added dropwise with stirring at 338 K under a N₂ atmosphere. The resulting slurry was allowed to age for 2 h, and the precipitate was removed by filtration and washed several times with deionized water followed by a single wash with ethanol. The precipitate was then dried for 10 h at 323 K in a vacuum oven to produce the precursor materials, denoted as CZAZ herein. Samples of this CZAZ precursor were calcined at 423, 573, 723 or 873 K for 6 h under a N₂ flow, to produce specimens denoted as CZAZ-423, CZAZ-573, CZAZ-723 and CZAZ-873, respectively.

For comparison purposes, a catalyst with the same composition was prepared by the co-precipitation method. After the co-precipitation resulting from combining metal nitrate and Na₂CO₃ solutions at 338 K and pH 7.0, the slurry was aged at 338 K for 2 h, followed by filtering, washing and drying. The dried product is denoted as cCZAZ, while cCZAZ-573 refers to the dried product after calcination for 6 h at 573 K under a N₂ flow.

2.2. Characterization

Powder XRD patterns were acquired using a Panalytical X'Pert Pro X-ray diffractometer with Cu K_α radiation, operating at 40 kV and 30 mA and in the step mode (0.0167°, 12 s). Specific surface areas were determined from N₂ adsorption-desorption isotherms at 77 K using a Micromeritics Tristar 3000 instrument. Thermogravimetric analysis (TGA) was performed with a SETSYS EVOLUTION TGA 16/18 instrument coupled to a mass spectrometer (OminStar, Pfeiffer Vacuum). Prior to analysis, the samples were first heated to 1000 K at 10 K/min in an Ar flow. Peaks at *m/z* = 18 and 44 were monitored because these resulted from the main pyrolysis products H₂O and CO₂, respectively. The morphology of each catalyst was analyzed by SEM with an FET XL 30S-FEG instrument at an accelerating voltage of 10.0 kV. XPS was performed using an AXIS ULTRA DLD spectrometer with a monochromatic Al K_α (1486.8 eV) source. The C 1s peak (284.6 eV) served as the reference to calibrate the binding energies.

TPR data were acquired using a quartz reactor in conjunction with a thermal conductivity detector (TCD) to determine the H₂ consumption. Each sample (50 mg) was initially heated at 423 K under Ar to remove moisture as well as other absorbed impurities and then reduced in a flow of 10 vol% H₂/Ar at a heating rate of 5 K/min up to 673 K. CO₂-TPD was conducted to assess the surface basic properties, employing a mass spectrometer (OminStar, Pfeiffer Vacuum). Prior to measurement, each sample (100 mg) was first activated at 503 K for 2 h under a feed gas (H₂:CO₂ = 3:1) and then saturated using a CO₂ flow at 323 K for 1 h. After flushing the physically adsorbed molecules from the catalyst with an Ar flow, CO₂-TPD was performed at a temperature ramp of 10 K/min under Ar up to 723 K. The amount of desorbed CO₂ was recorded by the mass spectrometer. The exposed Cu surface area (*S*_{Cu}) was determined by dissociative N₂O adsorption, using a TCD to monitor the consumption of H₂. Each sample (100 mg) was pretreated at 503 K under a flow of 10 vol% H₂/Ar for 2 h. The reduced sample was then cooled to 323 K and purged with Ar for 1 h, after which it was exposed to 5% N₂O/Ar for 1 h. Under these conditions, all exposed metallic copper was completely oxidized according to the reaction 2Cu(s) + N₂O → Cu₂O(s) + N₂, where Cu(s) represents surface Cu atoms. After cooling to room temperature under an Ar flow, the catalyst was reduced under a 10 vol% H₂/Ar flow using a temperature ramp of 5 K/min to heat the specimen from room temperature to 573 K. The amount of consumed H₂ is denoted as *n*_{H₂}. The *S*_{Cu} (m²/g) value was calculated according to the equations [17]: *S*_{Cu} = (*n*_{Cu} × *N*) / (1.4 × 10¹⁹ × *W*), where *S*_{Cu} is the exposed copper surface area per

gram catalyst, n_{Cu} is the amount of surface metallic copper on the catalyst ($n_{\text{Cu}} = 2n_{\text{H}_2}$), N is Avogadro's constant (6.02×10^{23} atoms/mol), 1.4×10^{19} is the number of copper atoms per m^2 , and W is the mass of the test sample.

2.3. Evaluation of catalysts

Activity measurements during the synthesis of methanol from CO_2/H_2 were carried out in a continuous flow, high pressure, fixed-bed reactor. In each trial, 1.0 g of the catalyst (40–60 mesh) was placed in a stainless steel tube reactor after dilution with an equal volume of quartz sand. The catalysts synthesized using the liquid reduction method were directly applied to activity measurements involving CO_2 hydrogenation to methanol with any further H_2 reduction. The reaction conditions included a temperature of 503–543 K, a pressure of 5.0 MPa, $n(\text{H}_2):n(\text{CO}_2) = 3:1$, and a gas hourly space velocity (GHSV) = 4600 h^{-1} . The catalyst obtained by co-precipitation was reduced under pure H_2 at atmospheric pressure and 503 K for 4 h prior to the activity tests. The products were quantitatively analyzed using gas chromatography (GC) in conjunction with a TCD. Gaseous products (H_2 , CO_2 , CO and CH_4) were assessed with a TDX-01 column while liquid products (H_2O and CH_3OH) were separated with a Porapak-Q column. The CO_2 conversion and the carbon-based selectivities for methanol and CO were calculated based on an internal normalization method. The space time yield (STY, $\text{g mL}^{-1} \text{ h}^{-1}$) for methanol, which gives the amount of methanol per mL catalyst per h, was calculated using the equation: $\text{STY} = (W \times X_{\text{CH}_3\text{OH}})/(t \times V)$, where W is the total mass of H_2O and methanol (g), $X_{\text{CH}_3\text{OH}}$ is the mass fraction of methanol, t is the reaction time (h), and V is the volume of catalyst (mL).

3. Results and discussion

3.1. Catalytic performance of the Cu/Zn/Al/Zr catalysts

The catalytic activities of the Cu/Zn/Al/Zr catalysts calcined at different temperature are summarized in Table 1. As can be seen, the CO_2 conversion increases while the methanol selectivity decreases as the reaction temperature is raised, a result that is consistent with other literature reports [18–20]. Methanol and CO are the main carbon-containing products under these reaction conditions. A higher reaction temperature evidently favors both activation and the conversion of CO_2 , because the reverse water gas shift (RWGS) reaction ($\text{CO}_2 + \text{H}_2 \rightarrow \text{CO} + \text{H}_2\text{O}$) is promoted to a greater extent than the synthesis of methanol ($\text{CO}_2 + 3\text{H}_2 \rightarrow \text{CH}_3\text{OH} + \text{H}_2\text{O}$). This occurs as a result of the en-

dothermic nature and higher apparent activation energy of the RWGS reaction [20]. In the case of those catalysts synthesized by liquid reduction, CO_2 conversion and methanol selectivity first increase and then decrease with increasing calcination temperature, and the CZAZ-573 exhibits the best catalytic performance. A maximum methanol STY value of $0.21 \text{ g mL}^{-1} \text{ h}^{-1}$ together with a CO_2 conversion of 24.5% and a CH_3OH selectivity of 57.6% are obtained over the CZAZ-573 at a reaction temperature of 543 K.

For comparison purposes, the cCZAZ-573 catalyst prepared by conventional co-precipitation was also assessed for activity. The superior CO_2 conversion of the CZAZ-573 catalyst relative to that of the cCZAZ-573 gradually becomes evident with increasing calcination temperature. In addition, the methanol selectivity of the CZAZ-573 is greater than that of the cCZAZ-573 at these three reaction temperatures. The higher activities of the catalysts made using the liquid reduction method are attributed to the presence of smaller copper particles and a larger quantity of basic sites; these effects have been discussed in detail in a previous research report [12].

3.2. Textural and structural properties

The XRD patterns of the Cu/Zn/Al/Zr catalysts are shown in Fig. 1. The diffraction peaks generated by the CZAZ precursor and calcined samples at $2\theta = 43.3^\circ$ and 50.4° correspond to the (111) and (200) planes of the Cu phase (JCPDS 04-0836). Characteristic diffraction peaks assignable to a Cu_2O phase (JCPDS 05-0667) are only observed in the calcined samples, implying that the Cu_2O phase in the CZAZ precursor is highly dispersed and so below the XRD detection, and that the dispersed Cu_2O particles tend to aggregate during calcination. These results suggest that the liquid reduction process reduces Cu^{2+} to Cu and Cu^+ . Diffraction peaks for the ZnO phase (JCPDS 36-1451) are observed, while Al_2O_3 and ZrO_2 are not evident as separate phases, and so may have been highly dispersed in amorphous forms or with very small particle sizes, or interacted with other metal oxides [21,22]. With increasing calcination temperature, the characteristic diffraction peaks ascribed to the Cu and Cu_2O phases exhibit an ongoing increase in intensity, owing to grain growth during the thermal treatment [23]. Notably, in the case of the CZAZ-873 sample, the intensity of the diffraction peak at $2\theta = 43.3^\circ$ assigned to Cu(111) planes increases dramatically, demonstrating that metallic Cu particles undergo dramatic growth at excessively high temperatures.

Fig. 2 presents the XRD patterns of the Cu/Zn/Al/Zr catalysts after the typical activation procedure (pretreated at 503 K

Table 1

Catalytic performance during CO_2 hydrogenation to methanol at different reaction temperature over various Cu/Zn/Al/Zr catalysts.

Sample	CO_2 conversion (%)			Selectivity for CH_3OH (C-mol%)			Selectivity for CO (C-mol%)			STY of CH_3OH ($\text{g mL}^{-1} \text{ h}^{-1}$)		
	503 K	523 K	543 K	503 K	523 K	543 K	503 K	523 K	543 K	503 K	523 K	543 K
CZAZ-423	15.2	19.8	21.3	59.4	57.6	52.9	40.6	42.4	47.1	0.14	0.18	0.18
CZAZ-573	17.3	22.0	24.5	62.1	60.9	57.6	37.9	39.1	42.4	0.16	0.20	0.21
cCZAZ-573	17.7	21.1	23.4	57.5	55.4	52.0	42.5	44.6	48.0	0.15	0.18	0.18
CZAZ-723	16.2	20.9	22.8	60.3	58.1	54.4	39.7	41.9	45.6	0.15	0.19	0.19
CZAZ-873	10.9	18.9	20.5	53.0	51.9	40.1	47.0	48.1	59.9	0.09	0.15	0.13

Reaction conditions: $P = 5.0 \text{ MPa}$, $n(\text{H}_2):n(\text{CO}_2) = 3:1$, $\text{GHSV} = 4600 \text{ h}^{-1}$.

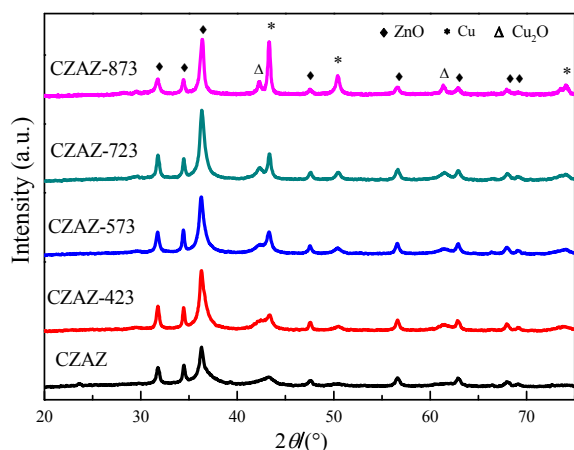


Fig. 1. XRD patterns of the Cu/Zn/Al/Zr catalysts.

with a feed gas). It can be seen that the characteristic Cu_2O diffraction peaks disappear, demonstrating that the catalysts undergo a secondary vapor phase reduction during the activation procedure. In addition, the intensity of the peaks attributed to the Cu phase increase significantly in comparison to that in Fig. 1, as a result of this secondary reduction and the aggregation of Cu particles during the high temperature treatment. The average Cu grain crystal sizes were calculated from the Cu(111) reflections using the Scherrer equation and were found to increase along with the calcination temperature (Table 2), indicating that the calcination temperature has a significant effect on the size of the metallic Cu particles.

As shown in Table 2, the specific surface area decreases from $52.0 \text{ m}^2/\text{g}$ for CZAZ-423 to $21.7 \text{ m}^2/\text{g}$ for CZAZ-873 with increasing calcination temperature. The growth of crystal grains and/or the agglomeration of particles at higher temperatures are responsible for the changes in the BET surface area and d_{Cu} [24]. The exposed Cu surface areas determined from N_2O dissociative adsorption measurements undergo a continuous decrease from CZAZ-573 to CZAZ-873, due to increasing aggregation of Cu particles. Interestingly, the CZAZ-423 sample has a relatively low S_{Cu} as a result of the high reduction temperature applied to this material (Fig. 6). This high temperature

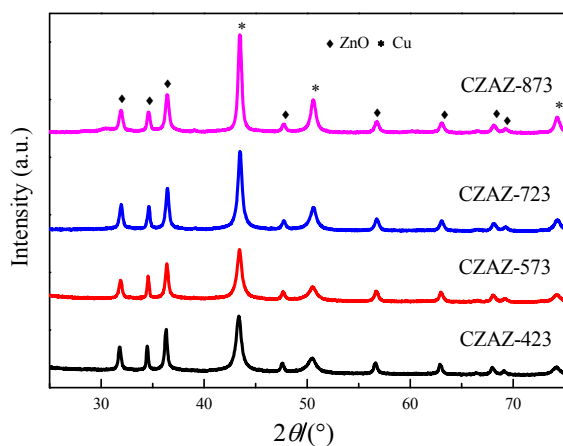


Fig. 2. XRD patterns of the Cu/Zn/Al/Zr catalysts after gas phase activation.

Table 2
Physicochemical properties of the Cu/Zn/Al/Zr catalysts.

Sample	BET surface area (m^2/g)	d_{Cu}^{a} (nm)	Cu surface area ^b (m^2/g)	$\text{Cu}^+/\text{Cu}^{0\text{c}}$ (%)
CZAZ-423	52.0	16.4	12.6	0.22
CZAZ-573	50.8	17.6	18.6	0.39
CZAZ-723	33.9	19.2	15.1	0.27
CZAZ-873	21.7	22.2	8.4	0.08

^a Calculated from Cu(111) reflections in XRD patterns (Fig. 2) using the Scherrer equation.

^b From N_2O dissociative adsorption measurements.

^c Calculated by Cu LMM Auger electron spectroscopy of the catalysts after activation under a feed gas at 503 K.

produces Cu species that are not fully reduced under the activation conditions.

To allow for further investigations of the thermal decomposition behaviors of these catalysts, the dried products obtained from both the liquid reduction and co-precipitation methods were assessed by TGA in conjunction with mass spectrometry (Fig. 3). The cCZAZ sample, having a zincian-malachite precursor structure [12], exhibits three mass loss peaks with a total mass loss of approximately 25.7%. There are labeled in the figure, where W1, W2 and W3 correspond to the loss of physisorbed water [25], zincian-malachite phase decomposition along with the release of H_2O and CO_2 , and the decomposition of stable Cu/Zn hydroxocarbonates [22] with only CO_2 release. In contrast, the CZAZ precursor undergoes a mass loss of about 12.9%. A broad H_2O peak is observed while little CO_2 is released during the thermal decomposition process, suggesting that hydroxy carbonates in this material are primarily transformed to metal/metal oxides during the liquid reduction process, in accordance with the XRD results in Fig. 1.

Fig. 4 presents SEM images of Cu/Zn/Al/Zr catalysts calcined at different temperatures. It can be seen that the catalysts are composed of either spherical or rod-like particles. With increasing calcination temperature, the spherical particles, with a size distribution in the range of 30–60 nm in the CZAZ-423, grow to 50–120 nm in the CZAZ-873. This result is in good agreement with the N_2 physisorption data. The rod-like particles are composed of the ZnO phase according to high resolution transmission electron microscopy (HRTEM) and scanning TEM-energy dispersive spectroscopy results [12]. These rods are approximately 300–500 nm in length. Instead of promoting strong interactions among each component, as occurs during the conventional co-precipitation method, the liquid reduction process results in the migration of Cu species from the co-precipitation slurry, such that the ZnO, undergoing less bonding, is inclined to grow into rod-like particles with good crystallinity.

3.3. XPS analysis

XPS data were acquired to determine the surface oxidation states of copper in these materials as well as their chemical compositions. Both Cu $2p_{3/2}$ and Cu $2p_{1/2}$ peaks are evident along with their satellite peaks in Fig. 5(a), indicating the pres-

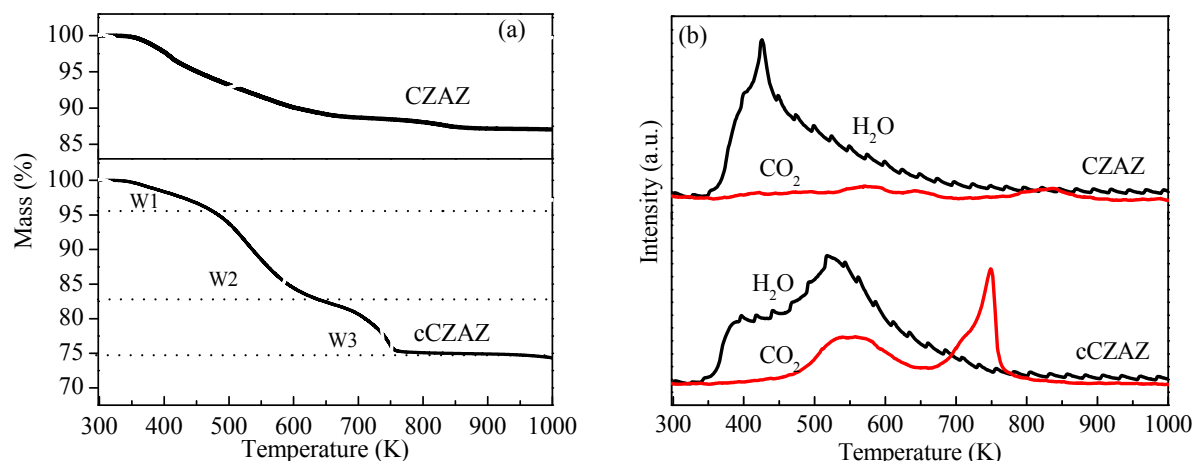


Fig. 3. (a) TG curves of Cu/Zn/Al/Zr precursors; (b) Mass spectra of the gaseous reduction products generated by these precursors.

ence of Cu²⁺ [23,26]. The characteristic binding energies of Cu 2p_{3/2} from Cu⁰, Cu⁺ and Cu²⁺ are located at 932.2–933.1, 932.0–932.8 and 933.2–934.6 eV, respectively [27]. It is noteworthy that the Cu 2p_{3/2} peaks are broad and bifurcated, which suggests that the catalysts possess more than one Cu species. These peaks can actually be deconvoluted into a large, narrow peak at 932.2 eV (attributed to Cu⁰ and/or Cu⁺ species) and a small, broad peak around 934.5 eV (assigned to Cu²⁺ species) [28]. Cu LMM Auger electron spectroscopy data were also acquired to assess the surface Cu valence states, as shown in Fig. 5(b). A principal peak with a broad profile is evident at about 916.8 eV, demonstrating that Cu⁺ is the predominant copper species on the surface, while peaks attributed to Cu²⁺ (917.9 eV) and Cu⁰ (918.8 eV) are indistinguishable owing to their low surface levels. The Cu²⁺ sites have evidently been completely reduced to Cu⁰ and/or Cu⁺ sites during the typical activation procedure, as evidenced by the absence of Cu 2p satellite peaks in Fig. 5(c). To distinguish between Cu⁰ and Cu⁺ species, the Cu LMM Auger electron spectroscopy data for activated catalysts

are presented Fig. 5(d). Here a principal peak at 918.8 eV (Cu⁰) and a smaller peak at 916.8 eV (Cu⁺) are observed. To assist in these investigations, the relative Cu⁺/Cu⁰ ratios of the catalyst surfaces were calculated and are presented in Table 2. These values increase in the order CZAZ-873 < CZAZ-423 < CZAZ-723 < CZAZ-573. Typically, Cu-based catalysts simultaneously contain Cu⁰ and Cu⁺ on their surfaces after reduction, and the Cu⁺ species may strongly interact with other components [28,29]. In the case of activated catalysts prepared by liquid reduction, these surface Cu⁺ species may result from the reduction of Cu²⁺ species strongly interacting with other metal oxides or may represent Cu⁺ species that are difficult to reduce to Cu⁰. The Cu⁰ species are from the readily reduced compounds CuO and Cu₂O. Thus, the value of Cu⁺/Cu⁰ can be an important indication of the interaction between Cu species and other metal oxides.

3.4. Reducibility of the Cu/Zn/Al/Zr catalysts

TPR measurements were carried out to study the reduction

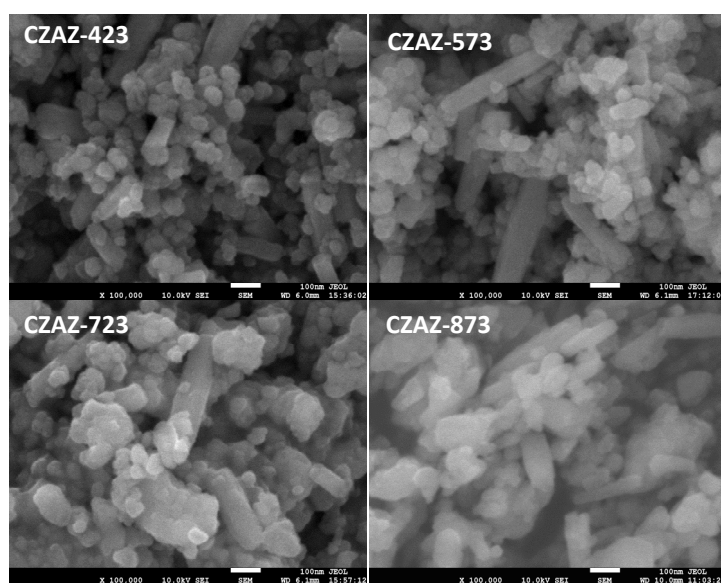


Fig. 4. SEM images of the Cu/Zn/Al/Zr catalysts.

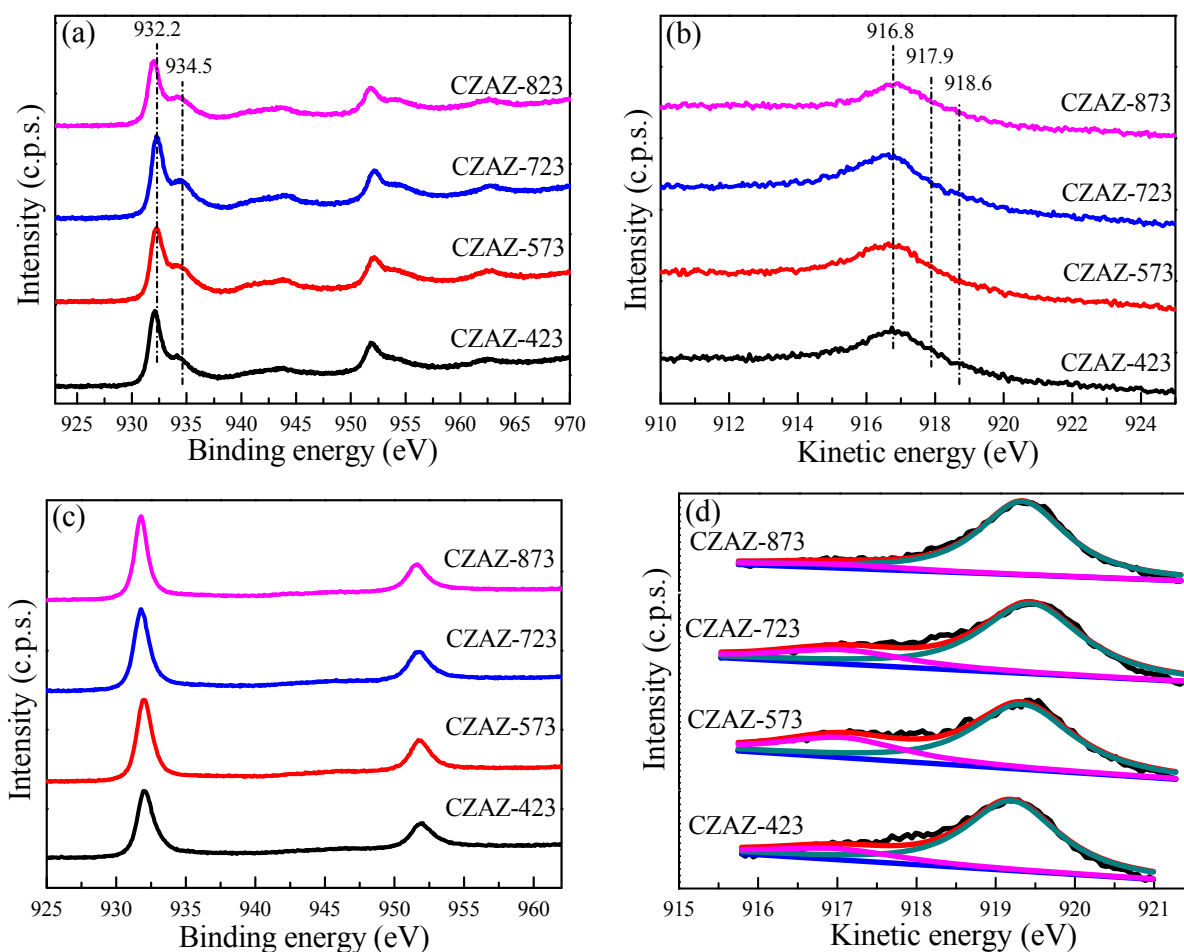


Fig. 5. Cu 2p spectra (a) and Cu LMM Auger electron spectra (b) of the Cu/Zn/Al/Zr catalysts; Cu 2p spectra (c) and Cu LMM Auger electron spectra (d) of the Cu/Zn/Al/Zr catalysts after activation under a feed gas.

behavior of the catalysts. As shown in Fig. 6, these samples generate a broad peak in the temperature range from 420 to 550 K, attributed to the reduction of CuO and Cu₂O. It can be seen that the catalysts prepared by the co-precipitation and liquid reduction methods show some differences in their reduction behavior. Compared with the cCZAZ-573 catalyst, the reduction peak area of the CZAZ-573 is decreased following

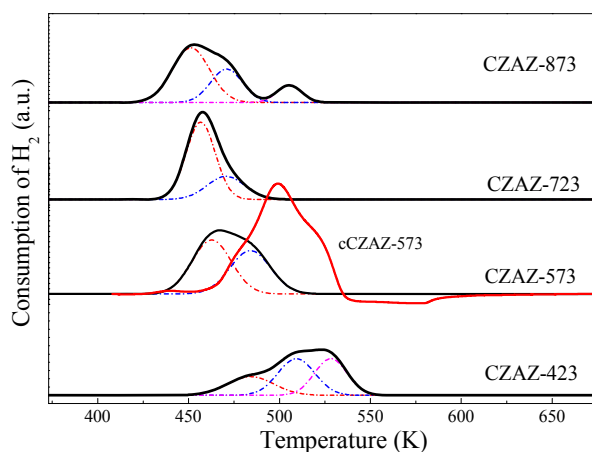


Fig. 6. TPR profiles of the Cu/Zn/Al/Zr catalysts.

liquid reduction, and its reduction temperature shifts to a lower temperature due to the weakened interactions in this material [12]. Catalysts obtained from liquid reduction and calcined at different temperature demonstrate that the initial reduction temperature shifts to lower values with increasing calcination temperature. Furthermore, the peak pattern becomes sharper and more symmetrical on going from 423 to 723 K. The broad peaks indicate the presence of several species or states, all being reduced at approximately the same temperature, whereas the sharp peaks demonstrate the existence of a single species or state. These changes in peak patterns likely reflect the effect of the high calcination temperature, which produces a more homogeneous distribution of Cu species [30].

3.5. Surface basicity of the Cu/Zn/Al/Zr catalysts

The CO₂ desorption profiles of the Cu/Zn/Al/Zr catalysts after the typical activation procedure are shown in Fig. 7. The profiles can be assigned to three scenarios representing three types of basic sites: weakly basic (surface OH⁻ groups), moderately basic (metal-oxygen pairs, such as Zn-O and Zr-O) and strongly basic (low coordination oxygen atoms) [31,32]. The differences in the positions of the desorption peaks among

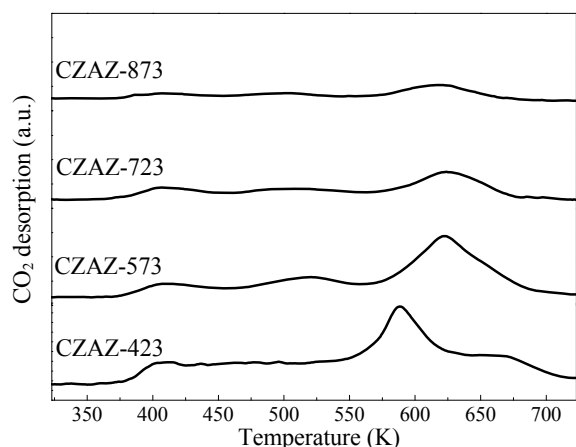


Fig. 7. CO₂-TPD profiles of the Cu/Zn/Al/Zr catalysts after the typical activation process under a feed gas.

these samples are minimal except in the case of the strongly basic sites of the CZAZ-423 sample, suggesting that calcination temperature has no significant effect on the strength of basic sites. However, an ongoing decrease in the amount of basic sites is observed with increasing calcination temperature, primarily attributed to a decrease in the specific surface area.

3.6. Long-term stability tests

Fig. 8 presents the long-term stability test data for the CZAZ-573 sample during the synthesis of methanol via CO₂ hydrogenation at 523 K, 5.0 MPa and a GHSV of 4600 h⁻¹. It can be seen that the CO₂ conversion and methanol selectivity obtained from the catalyst remain stable during a continuous 1000 h trial. These results demonstrate that the CZAZ-573 sample shows steady catalytic performance under the investigated reaction conditions.

Many researchers have pointed out that the activity of Cu-based catalysts during CO₂ hydrogenation to methanol is closely related to the exposed copper surface area (S_{Cu}) [19,20,30,33–37]. In this work, S_{Cu} was found to first increase and then decrease with increasing calcination temperature,

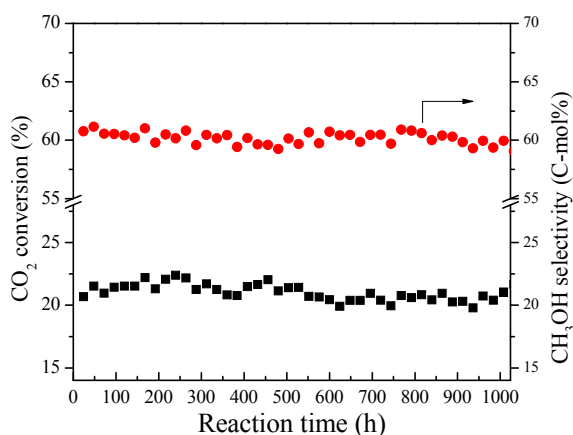


Fig. 8. Long-term stability test data for the CZAZ-573 catalyst over 1000 h. Reaction conditions: $P = 5.0$ MPa, $n(\text{H}_2):n(\text{CO}_2) = 3:1$, $T = 523$ K, GHSV = 4600 h⁻¹.

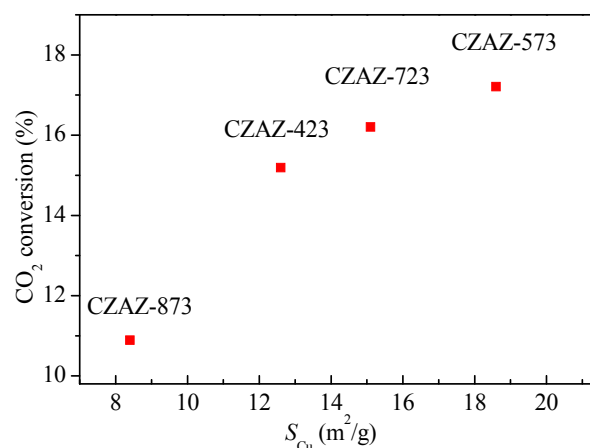


Fig. 9. The relationship between the CO₂ conversion and S_{Cu} . Reaction conditions: $P = 5.0$ MPa, $n(\text{H}_2):n(\text{CO}_2) = 3:1$, $T = 523$ K, GHSV = 4600 h⁻¹.

while CO₂ conversion showed a similar trend following the elevation of the calcination temperature, as shown in Fig. 9. However, the relationship between CO₂ conversion and S_{Cu} is not linear, a result that is consistent with other reports [38–40]. These results confirm that there must be some other factors affecting the catalytic performance during the synthesis of methanol from CO₂/H₂.

It is generally accepted that the coordination, chemisorption and activation of CO₂ and the homogeneous splitting of hydrogen take place on Cu⁰ and Cu⁺ [22,33,41–43]. Thus, Cu⁰ and Cu⁺ sites on the catalyst surface are important in determining the catalytic performance during CO₂ hydrogenation to methanol [33,41,42,44]. In comparison to Cu⁰ species, Cu⁺ species on the catalyst surface may represent electropositive sites that strongly interact with other components. As such, the Cu⁺/Cu⁰ ratio can be an important indicator of the interaction between Cu species and other metal oxides. In fact, it is well known that the RWGS reaction is promoted to a greater extent by metallic copper than by partially oxidized copper [41]. Toyir et al. [41] prepared Ga-promoted Cu-based catalysts with high selectivity for methanol production from CO₂/H₂ and attributed this selectivity to the presence of Cu⁺ species on the catalyst surface. Saito et al. [33] found that higher activities during methanol synthesis over a multicomponent Cu/ZnO-based catalyst were obtained when the value Cu⁺/Cu⁰ was approximately 0.7. In the case of the present Cu/Zn/Al/Zr catalysts prepared by liquid reduction with different calcination temperatures, the Cu⁺/Cu⁰ ratios (Table 2) first increase then decrease with increasing calcination temperature. The methanol selectivity exhibit a similar trend, further verifying that the Cu⁺/Cu⁰ value has a close relationship with methanol selectivity. Overall, a high value of Cu⁺/Cu⁰ achieved by selecting an appropriate calcination temperature is beneficial for the synthesis of methanol.

4. Conclusions

Cu/Zn/Al/Zr catalysts prepared by a liquid reduction method were found to contain three Cu valences (Cu²⁺, Cu⁺ and Cu⁰), although Cu⁺ was the predominant copper species de-

tectable on the surface of the precursor. The calcination temperature had a significant impact on the physicochemical properties. With increasing temperature, the specific surface area as well as the amount of basic sites decreased while the Cu particle size increased, due to higher rates of Cu aggregation. Furthermore, calcination temperature was found to affect the surface distribution and interaction of Cu species, thus leading to significant differences in reducibility and the Cu^+/Cu^0 value. These Cu/Zn/Al/Zr catalysts generated at different calcination temperatures were assessed during CO_2 hydrogenation to methanol, and the CZAZ-573 sample showed superior activity. A CO_2 conversion of 24.5% was obtained along with a methanol selectivity of 57.6% at 543 K. In addition, the CZAZ-573 sample exhibited higher activity than a cCZAZ-573 sample obtained using co-precipitation, especially with regard to methanol selectivity. A high exposed Cu surface area evidently favors CO_2 catalytic conversion while a high value of Cu^+/Cu^0 resulting from the use of an optimal calcination temperature is evidently helpful during the synthesis of methanol.

References

- [1] J. J. Wu, X. D. Zhou, *Chin. J. Catal.*, **2016**, 37, 999–1015.
- [2] G. A. Olah, A. Goepfert, G. K. S. Prakash, *J. Org. Chem.*, **2009**, 74, 487–498.
- [3] G. A. Olah, G. K. S. Prakash, A. Goepfert, *J. Am. Chem. Soc.*, **2011**, 133, 12881–12898.
- [4] M. Behrens, *J. Catal.*, **2009**, 267, 24–29.
- [5] O. Martin, J. Perez-Ramirez, *Catal. Sci. Technol.*, **2013**, 3, 3343–3352.
- [6] A. M. Cao, R. W. Lu, G. Vesper, *Phys. Chem. Chem. Phys.*, **2010**, 12, 13499–13510.
- [7] S. H. Zhu, X. Q. Gao, Y. L. Zhu, W. B. Fan, J. G. Wang, Y. W. Li, *Catal. Sci. Technol.*, **2015**, 5, 1169–1180.
- [8] L. Shi, W. Z. Shen, G. H. Yang, X. J. Fan, Y. Z. Jin, C. Y. Zeng, K. Matsu-da, N. Tsubaki, *J. Catal.*, **2013**, 302, 83–90.
- [9] X. M. Liu, G. Q. Lu, Z. F. Yan, J. Beltramini, *Ind. Eng. Chem. Res.*, **2003**, 42, 6518–6530.
- [10] S. Belin, C. L. Bracey, V. Briois, P. R. Ellis, G. J. Hutchings, T. I. Hyde, G. Sankar, *Catal. Sci. Technol.*, **2013**, 3, 2944–2957.
- [11] B. J. Liaw, Y. Z. Chen, *Appl. Catal. A*, **2001**, 206, 245–256.
- [12] X. S. Dong, F. Li, N. Zhao, F. K. Xiao, J. W. Wang, Y. S. Tan, *Appl. Catal. B*, **2016**, 191, 8–17.
- [13] Y. Tanaka, T. Utaka, R. Kikuchi, T. Takeguchi, K. Sasaki, K. Eguchi, *J. Catal.*, **2003**, 215, 271–278.
- [14] C. R. Jung, J. Han, S. W. Nam, T. H. Lim, S. A. Hong, H. I. Lee, *Catal. Today*, **2004**, 93–95, 183–190.
- [15] P. Djinić, J. Batista, A. Pintar, *Appl. Catal. A*, **2008**, 347, 23–33.
- [16] T. M. Ding, H. S. Tian, J. C. Liu, W. B. Wu, J. T. Yu, *Chin. J. Catal.*, **2016**, 37, 484–493.
- [17] Z. L. Yuan, L. N. Wang, J. H. Wang, S. X. Xia, P. Chen, Z. Y. Hou, X. M. Zheng, *Appl. Catal. B*, **2011**, 101, 431–440.
- [18] F. Arena, K. Barbera, G. Italiano, G. Bonura, L. Spadaro, F. Frusteri, *J. Catal.*, **2007**, 249, 185–194.
- [19] F. Arena, G. Mezzatesta, G. Zafarana, G. Trunfio, F. Frusteri, L. Spadaro, *J. Catal.*, **2013**, 300, 141–151.
- [20] X. M. Guo, D. S. Mao, G. Z. Lu, S. Wang, G. S. Wu, *J. Catal.*, **2010**, 271, 178–185.
- [21] M. W. Tan, X. G. Wang, X. X. Wang, X. J. Zou, W. Z. Ding, X. G. Lu, *J. Catal.*, **2015**, 329, 151–166.
- [22] P. Gao, F. Li, F. K. Xiao, N. Zhao, N. N. Sun, W. Wei, L. S. Zhong, Y. H. Sun, *Catal. Sci. Technol.*, **2012**, 2, 1447–1454.
- [23] Y. F. Zhu, X. Kong, D. B. Cao, J. L. Cui, Y. L. Zhu, Y. W. Li, *ACS Catal.*, **2014**, 4, 3675–3681.
- [24] X. M. Guo, D. S. Mao, G. Z. Lu, S. Wang, G. S. Wu, *Catal. Commun.*, **2011**, 12, 1095–1098.
- [25] G. Bonura, M. Cordaro, C. Cannilla, F. Arena, F. Frusteri, *Appl. Catal. B*, **2014**, 152–153, 152–161.
- [26] S. H. Zhu, X. Q. Gao, Y. L. Zhu, Y. F. Zhu, H. Y. Zheng, Y. W. Li, *J. Catal.*, **2013**, 303, 70–79.
- [27] J. Liu, C. H. Han, X. Z. Yang, G. J. Gao, Q. Q. Shi, M. Y. Tong, X. F. Liang, C. Li, *J. Catal.*, **2016**, 33, 162–170.
- [28] B. Zhang, Y. L. Zhu, G. Q. Ding, H. Y. Zheng, Y. W. Li, *Appl. Catal. A*, **2012**, 443–444, 191–201.
- [29] A. Dandekar, M. A. Vannice, *J. Catal.*, **1998**, 178, 621–639.
- [30] S. Natesakhawat, J. W. Lekse, J. P. Baltrus, P. R. Ohodnicki, B. H. Howard, X. Y. Deng, C. Matranga, *ACS Catal.*, **2012**, 2, 1667–1676.
- [31] G. D. Wu, X. L. Wang, W. Wei, Y. H. Sun, *Appl. Catal. A*, **2010**, 377, 107–113.
- [32] P. Gao, F. Li, H. J. Zhan, N. Zhao, F. K. Xiao, W. Wei, L. S. Zhong, H. Wang, Y. H. Sun, *J. Catal.*, **2013**, 298, 51–60.
- [33] M. Saito, T. Fujitani, M. Takeuchi, T. Watanabe, *Appl. Catal. A*,

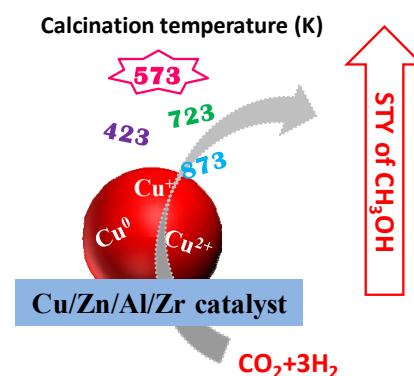
Graphical Abstract

Chin. J. Catal., 2017, 38: 717–725 doi: 10.1016/S1872-2067(17)62793-1

CO_2 hydrogenation to methanol over Cu/Zn/Al/Zr catalysts prepared by liquid reduction

Xiaosu Dong, Feng Li*, Ning Zhao, Yisheng Tan, Junwei Wang, Fukui Xiao
 Institute of Coal Chemistry, Chinese Academy of Sciences;
 University of Chinese Academy of Sciences;
 National Engineering Research Center for Coal-based Synthesis

Cu/Zn/Al/Zr catalysts containing Cu^{2+} , Cu^+ and Cu^0 were prepared via a liquid reduction method and then calcined at different temperatures. These materials were subsequently applied to the synthesis of methanol by the hydrogenation of CO_2 to assess the effects of varying the calcination temperature.



- 1996, 138, 311–318.
- [34] W. X. Pan, R. Cao, D. L. Roberts, G. L. Griffins, *J. Catal.*, **1988**, 114, 440–446.
- [35] H. J. Zhan, F. Li, P. Gao, N. Zhao, F. K. Xiao, W. Wei, L. S. Zhong, Y. H. Sun, *J. Power Sources*, **2014**, 251, 113–121.
- [36] X. M. Guo, D. S. Mao, G. Z. Lu, S. Wang, G. S. Wu, *J. Mol. Catal. A*, **2011**, 345, 60–68.
- [37] P. Gao, F. Li, N. Zhao, F. K. Xiao, W. Wei, L. S. Zhong, Y. H. Sun, *Appl. Catal. A*, **2013**, 468, 442–452.
- [38] T. Witoon, T. Permsirivanich, W. Donphai, A. Jaree, M. Chareonpanich, *Fuel Process. Technol.*, **2013**, 116, 72–78.
- [39] L. Li, D. S. Mao, J. Yu, X. M. Guo, *J. Power Sources*, **2015**, 279, 394–404.
- [40] Q. Sun, Y. L. Zhang, H. Y. Chen, J. F. Deng, D. Wu, S. Y. Chen, *J. Catal.*, **1997**, 167, 92–105.
- [41] J. Toyir, P. R. de la Piscina, J. L. G. Fierro, N. Homs, *Appl. Catal. B*, **2001**, 34, 255–266.
- [42] J. Toyir, P. R. de la Piscina, J. L. G. Fierro, N. Homs, *Appl. Catal. B*, **2001**, 29, 207–215.
- [43] G. C. Chinchén, K. C. Waugh, *J. Catal.*, **1986**, 97, 280–283.
- [44] G. C. Wang, Y. Z. Zhao, Z. S. Cai, Y. M. Pan, X. Z. Zhao, Y. W. Li, Y. H. Sun, B. Zhong, *Surf. Sci.*, **2000**, 465, 51–58.